NATIONAL INSTITUTE FOR NUCLEAR AND HIGH ENERGY PHYSICS

ASR-D-005

Structural Analyses of the AMS-TTCS Evaporator Assembly

Abstract

This report shows the outcome of the stress, frequency and thermal expansion calculation of the TTCS evaporator assembly. The evaporator assembly contains the loop, the support brackets and the thermal bars.

Corijn Snippe
Bart Verlaat

First Draft , 18 February 2005

Change Log:
Issued: *18 February 2005*
Revision -:

NIKHEF
P.O.BOX 41882, NL 1009 DB AMSTERDAM
THE NETHERLANDS

Summary

This report summarizes the structural analyses done on the evaporator section of Tracker Thermal Control System. The analyses include the verification of the thermal bar assemblies, the evaporator tubes and the evaporator support brackets. It reports on the structural verification of launch, thermal and installation forces. Also Natural frequency analyses are included.

1 Mechanical Design overview.

The TTCS evaporator is a serial cooling loop with soldered cooling blocks. The several sections are welded together with orbital and laser welding. The cooling blocks are thermally connected to the thermal bars of the tracker.

The mechanical design of the thermal bars can be reviewed via the drawing tree which is available on the internet at:
http://www.nikhef.nl/pub/departments/mt/projects/ams/SiTracker/ASC13.html

The mechanical design of the evaporator loop can be reviewed at:
http://www.nikhef.nl/pub/departments/mt/projects/ams/SiTracker/ASM28.html

The mechanical design of the brackets supporting the evaporator can be reviewed at:
http://www.nikhef.nl/pub/departments/mt/projects/ams/SiTracker/ASM56.html

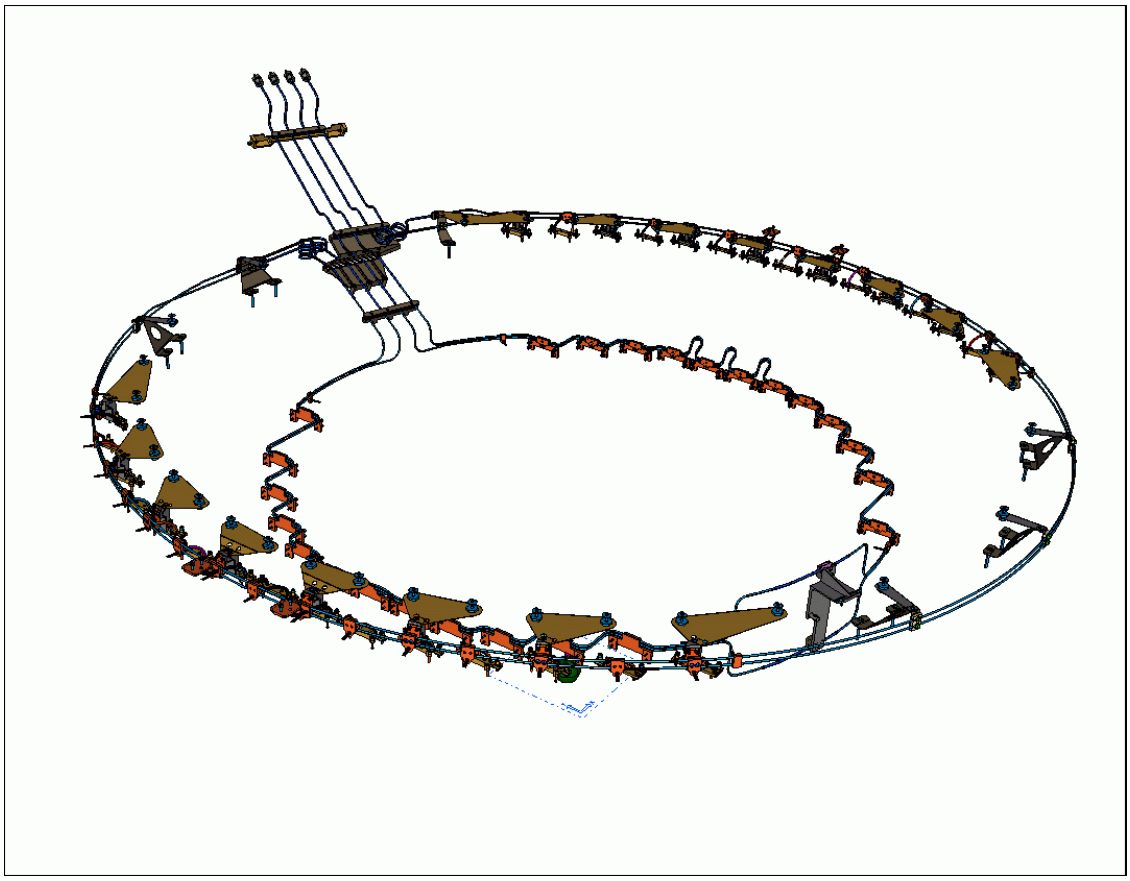

Figure 1.1 Total assembly of the evaporator loop

2 Finite Element Model overview

2.1 Thermal bar model

Many of the components which make up the thermal bar have been modeled as either solid elements or thin shell elements, as can be seen in figure 2.1. The X- and Y-direction match the strong directions of the TPG material, the Z-direction is the weak direction of this material. From experience we know that this material behaves in a strange way. Because of the very big difference in stiffness properties in the stiff X-Y compared to the Z-direction, it does not give the stiffness to the construction as it would result from calculations in which these properties have been added. Therefore, calculations with the TPG material have been performed, as well as without this material. The latter calculation can be interpreted as a worst case situation for the aluminium, this material has to carry then all the load. Please note that if the TPG has been neglected in the calculations, this is only true for the stiffness, to account for the mass of it, the density of the aluminium has been adjusted to compensate for the loss of mass of the TPG.

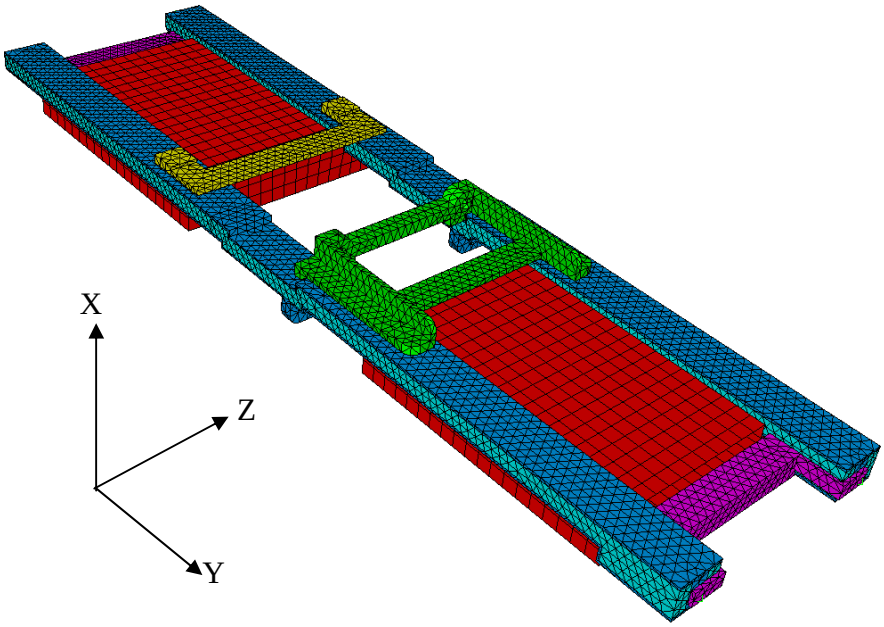

Figure 2.1: Finite element model of the thermal bar. The conductor, base, clip support and connector bridges have been modeled using solid elements, the hybrid boxes are modeled using shell elements and the thermal connectors are represented by lumped masses at the end of the thermal conductors.

There is a small difference in the design of the thermal bar of plane 2 and 4 compared to the bar of plane 3. The geometry is similar; the mounting on the ends of the bar is different. The plane 2&4 thermal bars have an evaporator copper bridge attached, while the plane 3 thermal bar have only the flex connectors attached. The analyses is only done on a plane 2&4 thermal bar, since this is considered to be the worst load case due to the heavier thermal bridge.

.

2.2 Evaporator model

The cooling loop is fixed with flexibility to the Tracker and the thermal bars. The brackets holding the springs of the outer loop are not modeled because they are assumed to be strong enough. Due to the spring they are not part of the evaporator structural behavior. They are only carrying the weight of the loop which is very light. The parts which will be used in the simulation model, are depicted in figure 2.2. In all analyses, holes where these parts are fixed to the rest of the detector with bolts will be fully constraint.

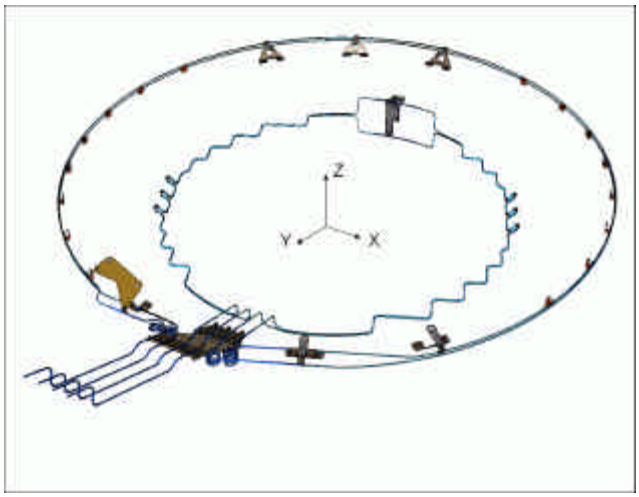

Figure 2.2. Assembly necessary for the analysis of the Cooling Loop System.

Cooling pipes have been meshed with beam elements in the larger part of the model, only in the neighborhood of the Flange Exit Clamp Base, shell elements have been used. Supports and Leaf Springs have been meshed with shell elements and both Clamp Bases consist of 3D tetrahedral elements, see figure 2.3. All elements used in the model are of the quadratic type.

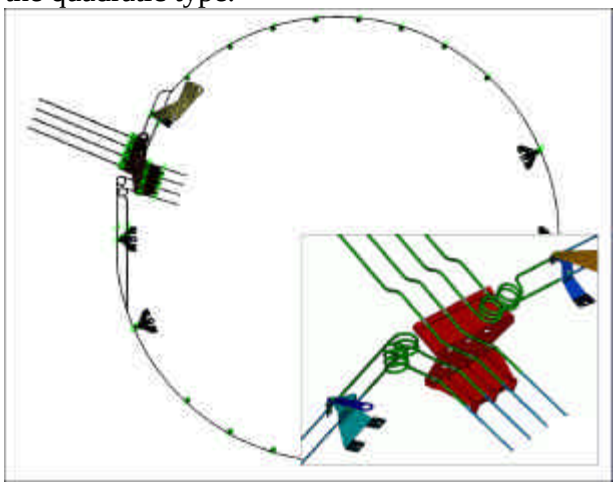

Figure 2.3. FE model of the outer loop generated from the I-deas CAD model shown in figure 2.2.

3. Launch and landing load stress analyses.

In order to survive launch and landing, the evaporator assembly must withstand a 40g in any direction with 10g in the 2 perpendicular directions. The Safety factor for yield must be 1.25, the ultimate safety factor must be 2. The Margin of safety, which is the margin from the safety factor is the value which need to be communicated with NASA/LMCO. For the margin of safety counts:

$$MSy = \frac{FTy}{FSy * f} - 1 \qquad MSu = \frac{FTu}{FSu * f} - 1$$

MSx=Margin of safety for yield or ultimate
FSx=Factor of safety for yield or ultimate
FTx=Ultimate or Yield stress
f=Maximum limit stress
u=ultimate
y=yield

This value must be positive to meet the launch and landing load requirements. Table 3.1 show the stress analyses results of the Launch and landing load analyses.

Discription	Part number	Material	Load factor	Maximum Limit Stress (N/mm2)	Fty (N/mm2)	Ftu (N/mm2)	Msy	Msu
		AL6082		120	240	300	0.60	0.25
	AMSII144A2 /	TPG TC1050 x,y		13.9	NA	3900	NA	139.29
P24/P3 Thermal Bar	AMSII145A2	TPG TC1050 z	40g,10g,10g	0.099	NA	0.4	NA	1.02
Evaporator tube	ASM28, ASM29	CRES 316L	40g,10g,10g	79.5	319	632	2.21	2.97
Central clamp	ASM25	AL6082	10g,10g,40g	37.7	240	300	4.09	2.98
Flange exit clamp	ASM06	AL6082	10g,10g,40g	80	240	300	1.40	0.88
Outer ring support 1	ASM39	AL6082	40g,10g,10g	48	240	300	3.00	2.13
Outer ring support 2	ASM57	AL6082	10g,40g,10g	83	240	300	1.31	0.81
Outer ring support 3	ASM62	AL6082	10g,10g,40g	125	240	300	0.54	0.20
Spring support	ASM1901	AL6082	40g,10g,10g	64	240	300	2.00	1.34

Table 3.1: Summary of stress analyses

3.1. Thermal bars stress analyses

The worst case acceleration load is the load in X. This will be 40g in X-direction and 10g in both the Y- and Z-direction. In the first calculation a course mesh has been used as can be seen in figure 3.1. The highest stresses are expected at the bolt hole connections to the sandwich planes or at the connections between the TPG material and the surrounding

aluminum. The result of the stress calculation can be seen in Figure 3.2. Units of the stress values in the plots are in mN/mm².

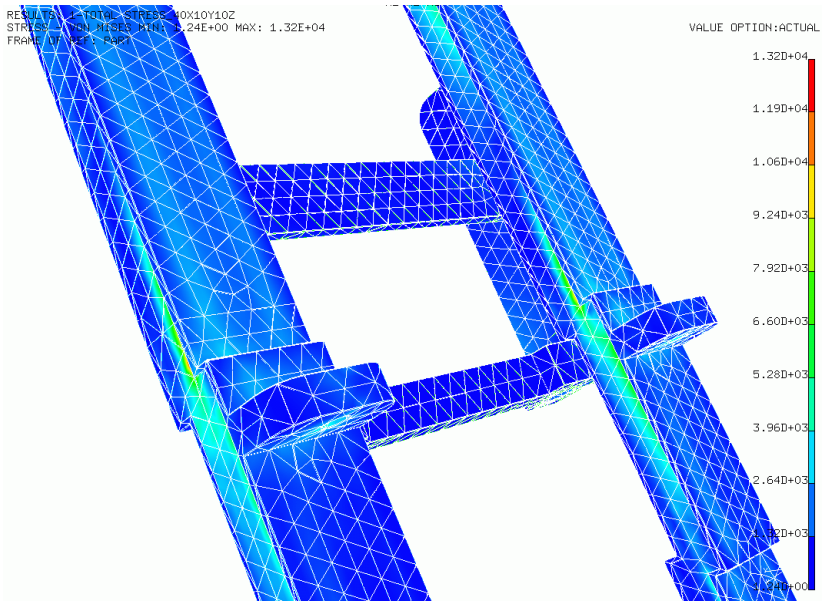

Figure 3.1. Von Mises stresses in the thermal bar due to the (40,10,10)g acceleration loadt.

The highest von Mises stresses occur in the TPG material in the neighborhood of the bolt holes (13.2 MPa / 1916 psi). The highest stress at a bolt hole is 4.8 MPa. Because TPG is a very brittle material and also orthotropic, the principal stresses are a better indicator, also the stress in the weak direction of the material. The highest principal stress in the TPG is 13.9 MPa (2018 psi), the highest stress in the weak direction (Z) is 0.098 Mpa (14 psi). Because the mesh in the neighborhood of the highest stresses is quite coarse, a more detailed calculation has been performed, including the highest stress regions and the bolt holes. The FE model for the detailed calculation can be seen in Figure 3.2.

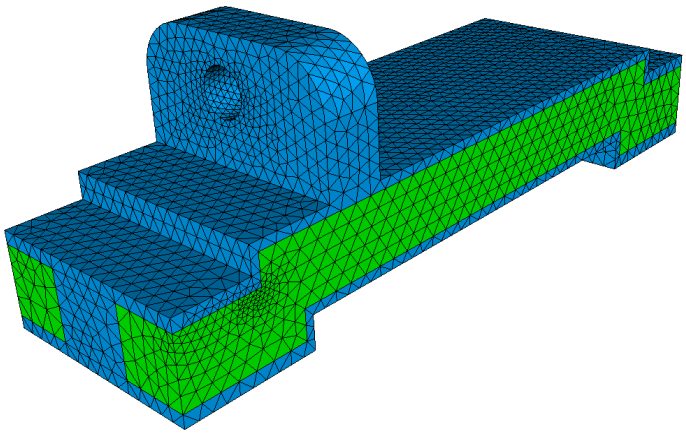

Figure 3.2. Finite Element model of a small portion of the thermal bar

Figure 3.3 shows the maximum principal stresses, the highest value is 13.7 Mpa (1990 psi), the maximum stress in the weak direction (Z) is 0.099 MPa (14 psi).

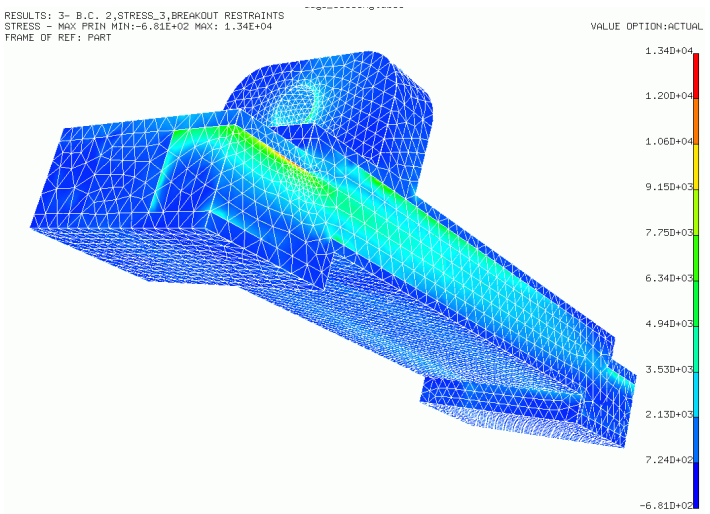

Figure 3.3. Maximum principal stresses in the detailed model for stress analysis.

For checking reasons, also a gravity load has been applied with an acceleration of 40g in the Y-direction and 10g in the other directions. This calculation resulted in lower stresses and reaction forces. Figure 3.4 shows the maximum stress in the thermal bar if the TPG material is neglected. As mentioned earlier, this situation is a worst case for the aluminium. Leaving the TPG out leads to much higher stresses, the deflection is much higher. A simple calculation shows that the stiffness value EI of the cross section of the thermal bar with TPG is about 45 times higher than without TPG. The maximum stress is 120 MPa (17.4 ksi). The yield stress for the aluminium is 240 MPa, the ultimate stress is 300 MPa, so the bar without TPG can withstand the loads.

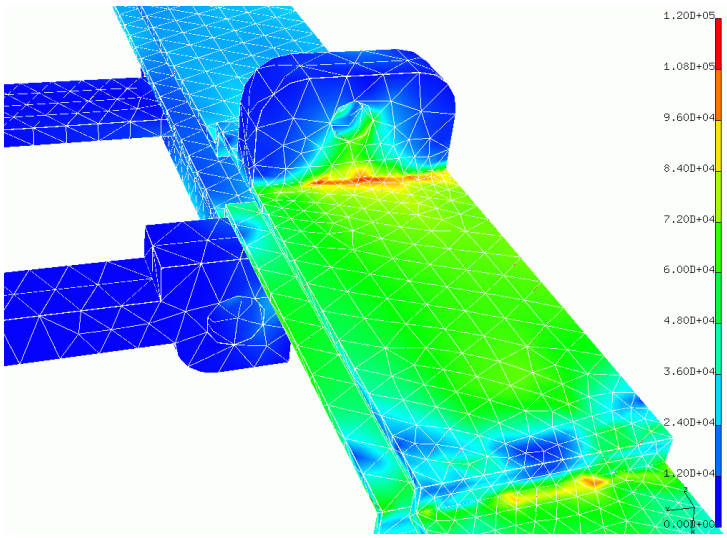

Figure 3.4. Stress calculation of the thermal bar without TPG shows a maximum stress of 120 MPa.

3.2. Evaporator stress analyses

The worst case direction in which the 40g acceleration acts on the evaporator assembly, can differ from part to part. The most flexible way to analyse this situation is to construct three loads of 1g each in the three orthogonal directions and analyse the assembly with all these three load cases. Assumed that the deformations and stresses scale linearly with the acceleration (i.e. no large deformations are present and no plastic deformation will occur) the worst case situation can be found by multiplying the results in one direction with a factor 40, and adding the results in the other directions multiplied with a factor 10.

The stresses in the Central Evaporator Clamp Base are highest if the acceleration of 40 g is directed normal to the cooling tube planes (Z), this (von Mises) stress is about 38 MPa, see figure 3.5.

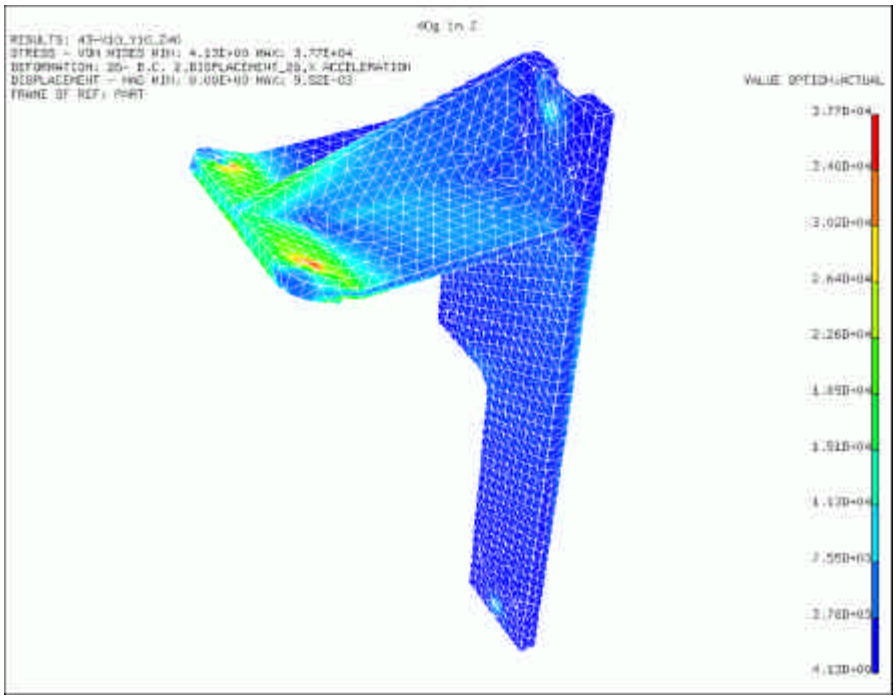

Figure 3.5. The maximum stress in the Central Evaporator Clamp Base is 37.7 MPa.

The stresses in the cooling tubes can be up to 80 MPa, here the worst case acceleration is in the X direction, see figure 3.6. The highest stress in the cooling pipes occur in the neighborhood of the Central Evaporator Clamp Base, in a relatively sharp bend.

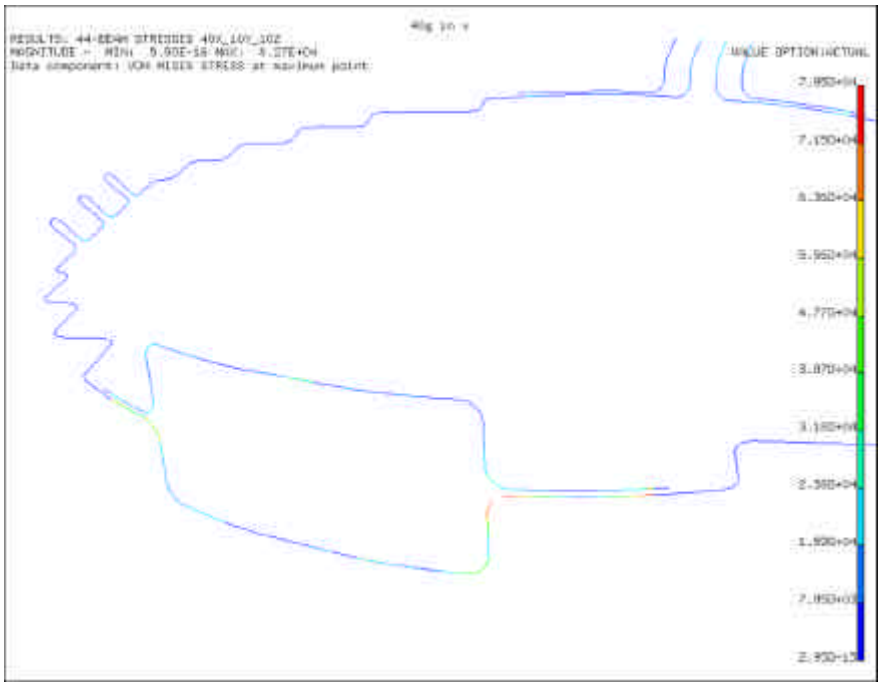

Figure 3.6. The maximum stress in the cooling pipes will be 79.5 MPa during launching.

On the other side, close to the Flange Exit Clamp Base, the highest stress in the cooling tubes are slightly lower, about 70 MPa in the exit tube (shown in figure 3.7) in the Z direction.

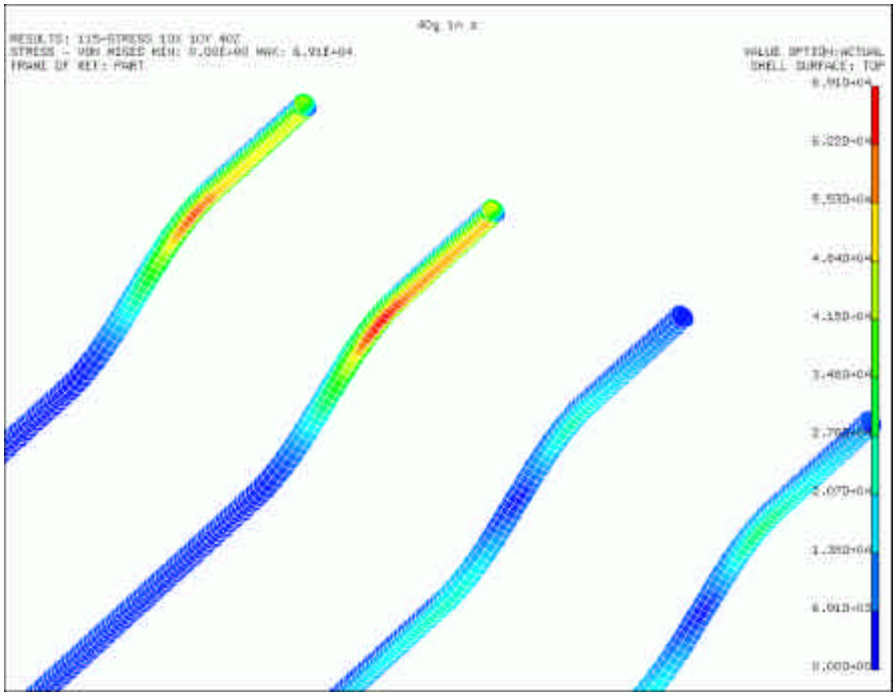

Figure 3.7. The maximum stress in the cooling pipes close to the Flange Exit Clamp Base will be 69.1 MPa during launching.

Figure 3.8, at last, shows the von Mises stresses in the Flange Exit Clamp Base itself, being about 80 MPa in a very small area, with most of this part being in a low stress situation.

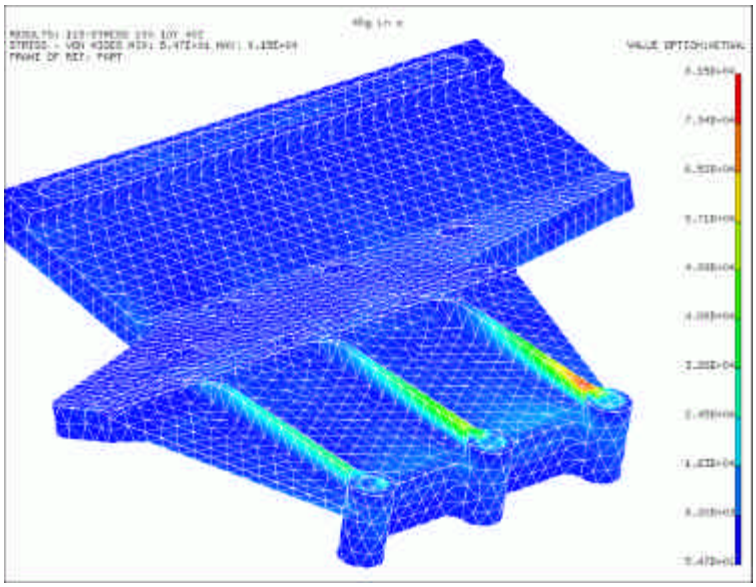

Figure 3.8. The maximum stress in the Flange Exit Clamp Base.

All the stresses calculated in this section, are tolerable.

4. Frequency analyses

4.1. Thermal bars

To get a feeling of the order of the results with respect to the frequency analysis, a simple hand calculation can be done in which the thermal bar is assumed to be fixed in the middle. The length of one end is then 138 mm, the mass of one thermal bar conductor on one side of the fixing with all components included is about 100 grams. The bending stiffness of the beam E·I can be calculated from the bending stiffness of the separate materials (aluminum and TPG), the resulting value is 45 Pa·m^4.
According to [1], the first resonance frequency for a one-end fixed beam with uniform mass is:

$$f = \frac{1}{2p} \cdot \sqrt{\frac{140}{11} \cdot \frac{EI}{mL^4}}$$

in which m is the uniform mass per unit length and L is the length of the beam. Filling in the appropriate values gives a first resonance frequency of 234 Hz.

The FE model used for the stress analysis has been changed a little bit: some components have been added as a lumped mass on the thermal bar conductor, the components that have been modeled besides the conductor are the base and the clip support, see Figure 4.1.

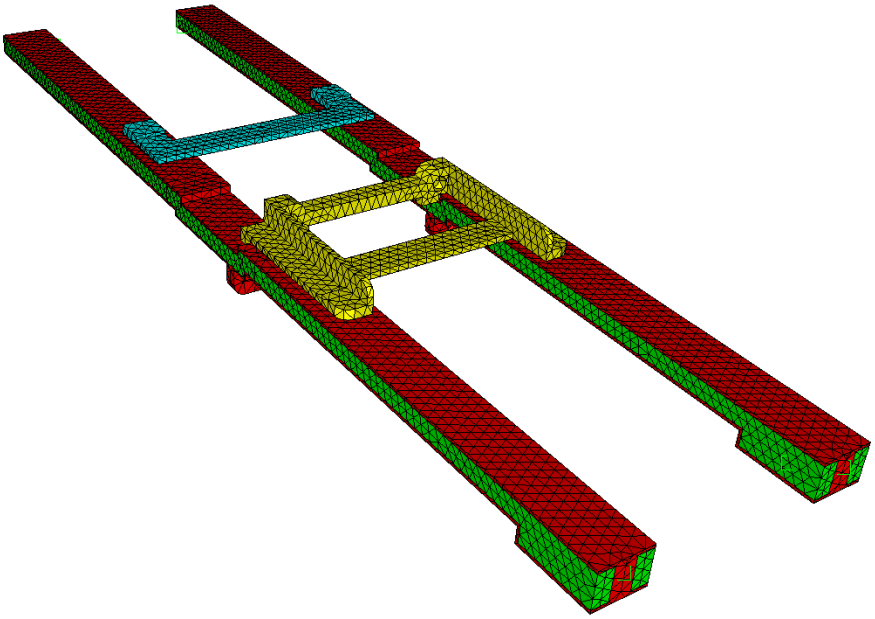

Figure 4.1. Adjusted FE model used for the frequency analysis. Besides the thermal bar conductor also the base (yellow elements) and the clip support (cyan elements) have been modeled.

[1] Ray W. Clough and Joseph Penzien: Dynamics of Structures, second edition, 1993, Mc Graw Hill.

In the first calculation, the TPG material is present in the model. It shows that the first resonance frequency of this structure is 149 Hz, but this is not a possible mode shape (see Figure 4.2), because the hybrid boxes, which have now been represented as lumped masses) will prevent the two conductors to move in opposite directions.

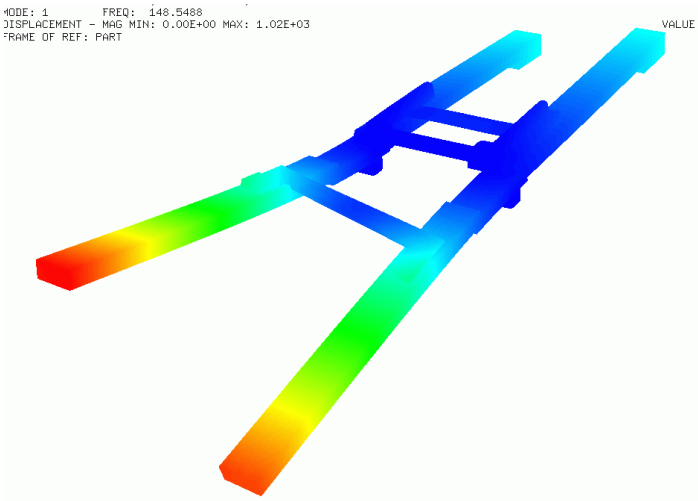

Figure 4.2. The first resonance frequency of the used FE model, which doesn't represent a possible mode shape.

The second mode shape, however, is possible (see Figure 10), the resonance frequency is slightly higher than the first one, namely 152 Hz.

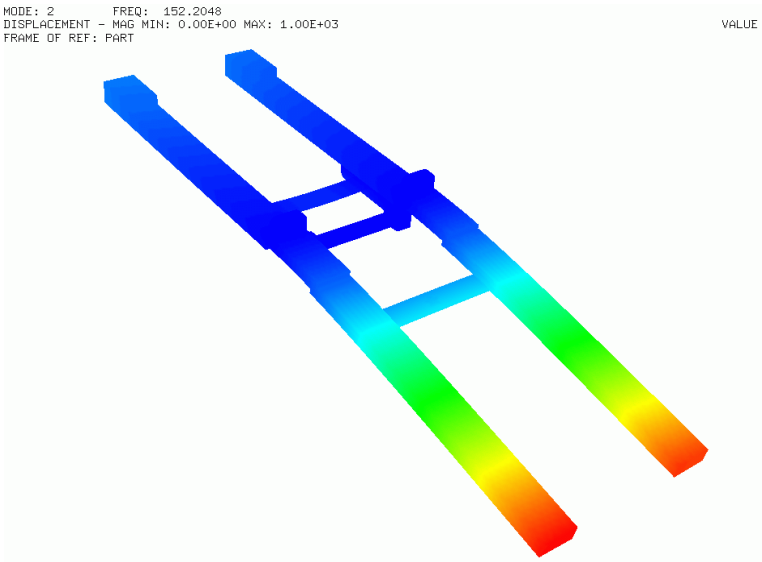

Figure 4.3. The first possible mode shape, which has a frequency of 152 Hz.

In reality, the frequency of this mode shape will be somewhat higher, because the hybrid boxes, which have a certain stiffness, will force the mode shape in a slightly different way. The value of 152 Hz can thus be interpreted as a worst case situation.

Also a frequency analysis has been performed when the TPG material is neglected. This means in the next calculation that the mass of the TPG is put into the aluminium by giving it a higher density. The results show a first calculated resonance frequency of 80 Hz, see figure 11.

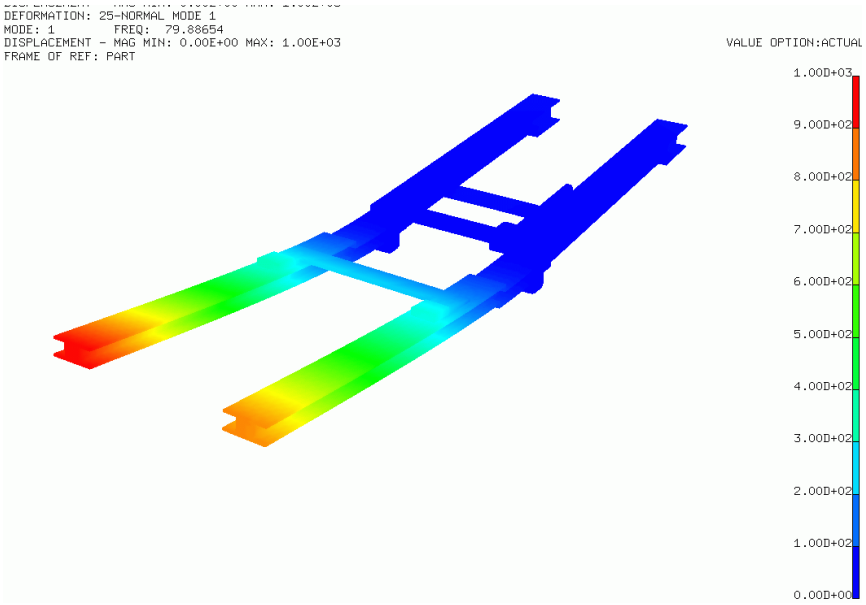

Figure 4.4. First resonance frequency shape of the thermal bar without TPG.

This is what also comes out of the vibration tests done with the thermal bars [see: AMS-02 vibration tests of tracker components, performed by the AMS group, DPNC – University of Geneva, Switzerland], the first resonance frequency has been detected at 84 Hz.

4.2. Evaporator loop

The analysis shows that the three lowest resonance frequencies all lie in the range between 100 and 110 Hz, with 100.6 Hz being the lowest in the cooling pipes, see figure 4.5. The other two resonance frequencies mentioned can be seen in figure 4.6 and 4.7, being 104.4 Hz in the cooling pipe spiral and 107.0 Hz in the Central Evaporator Clamp Base, respectively.

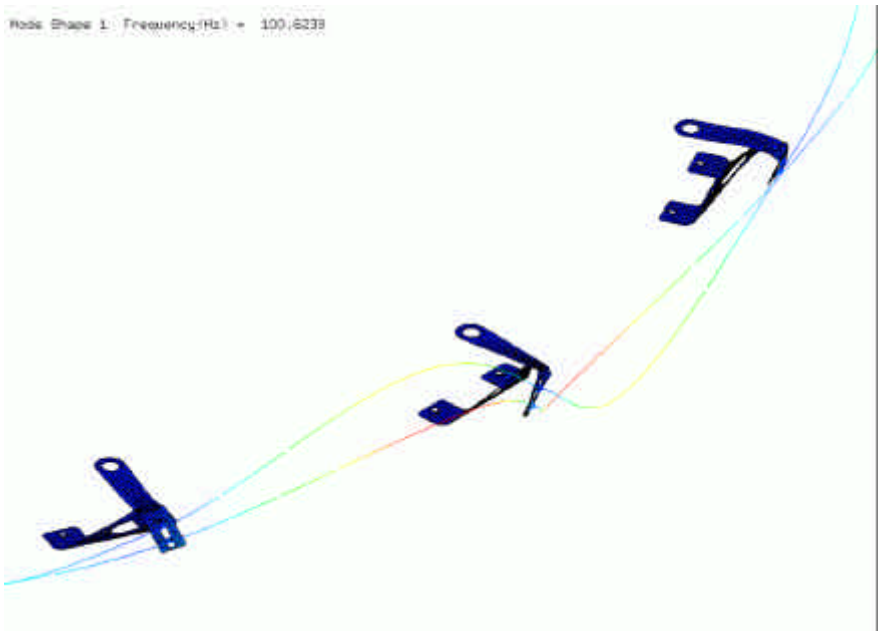

Figure 4.5. The first resonance frequency in the cooling pipes has a value of 100.6 Hz.

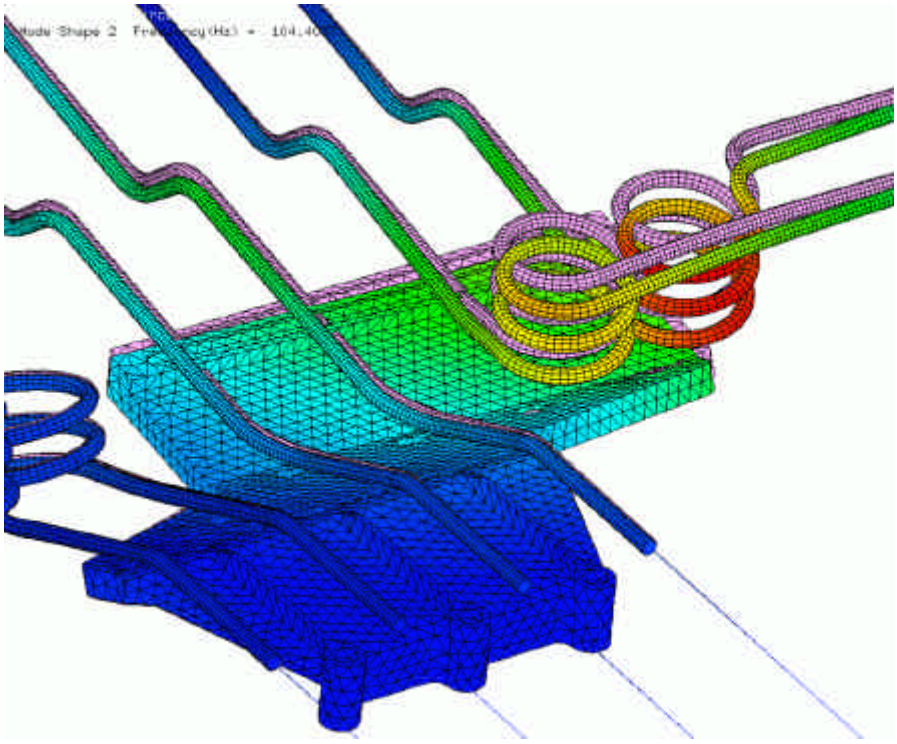

Figure 4.6. The first resonance frequency in the cooling pipe spiral has a value of 104.4 Hz.

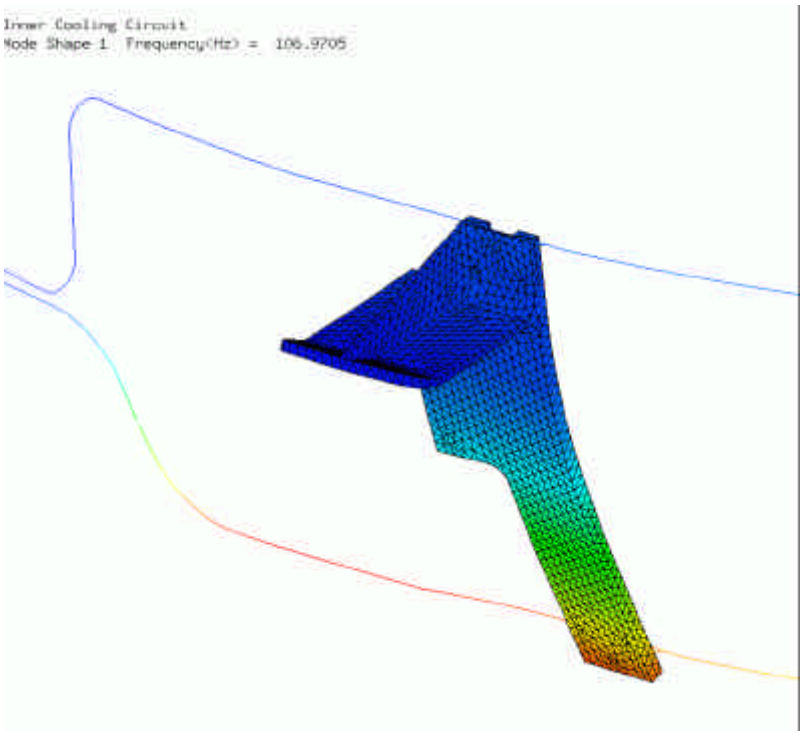

Figure 4.7. The first resonance frequency in the Central Evaporator Clamp Base has a value of 107.0 Hz.

5. Displacements resulting from a 60 K temperature drop

The difference in temperature between assembling conditions and working conditions can rise up to 60 K (from +20 ºC to -40 ºC). The temperature of -40 ºC will be the working temperature of the cooling pipes, contraction of the pipe material will lead to displacements and stresses in the assembly. Figures 5.1-5.3 show the displacements of the cooling pipes themselves (maximum 1.8 mm) and of both Clamp Bases.

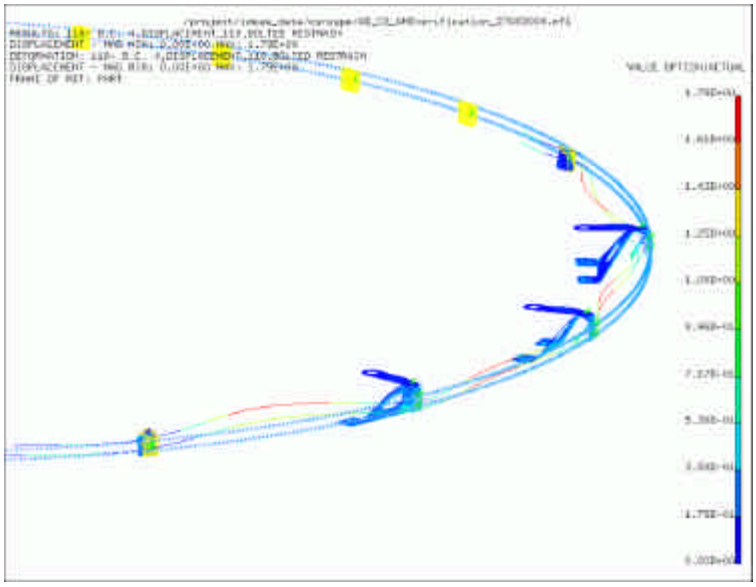

Figure 5.1 Maximum deformation of the cooling pipes resulting from a 60 K temperature change is 1.79 mm.

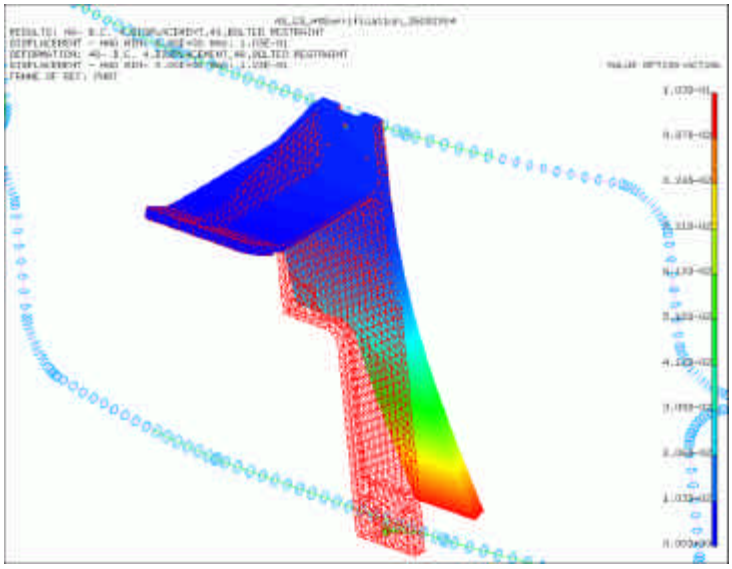

Figure 5.2. Maximum deformation of the Central Evaporator Clamp Base resulting from a 60 K temperature change is 0.1 mm.

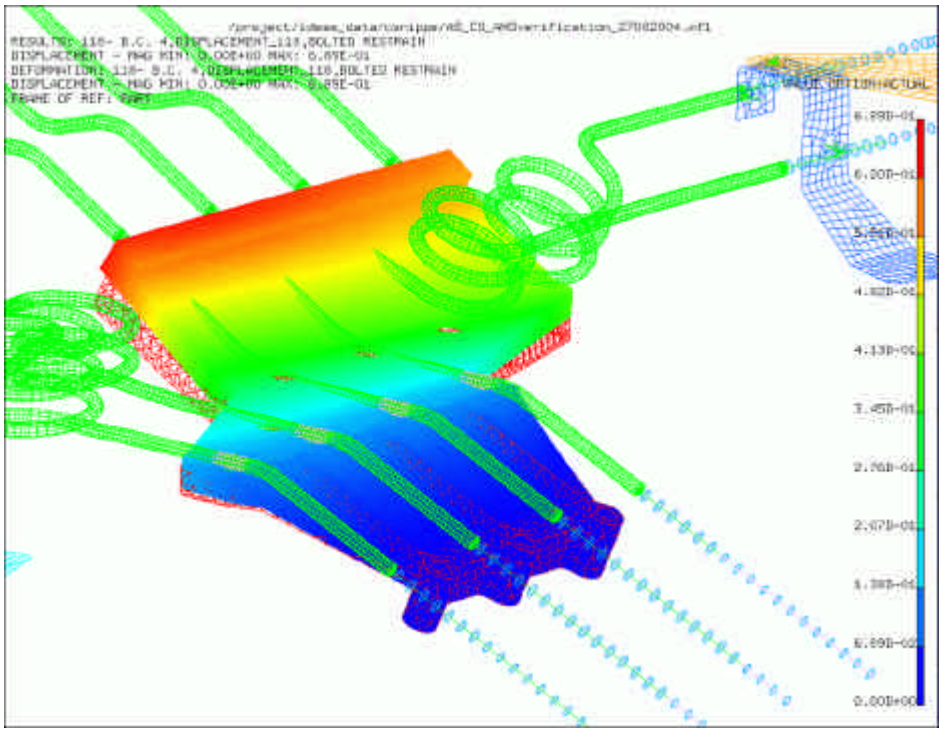

Figure 5.3 Maximum deformation of the Flange Exit Clamp Base resulting from a 60 K temperature change is 0.69 mm.

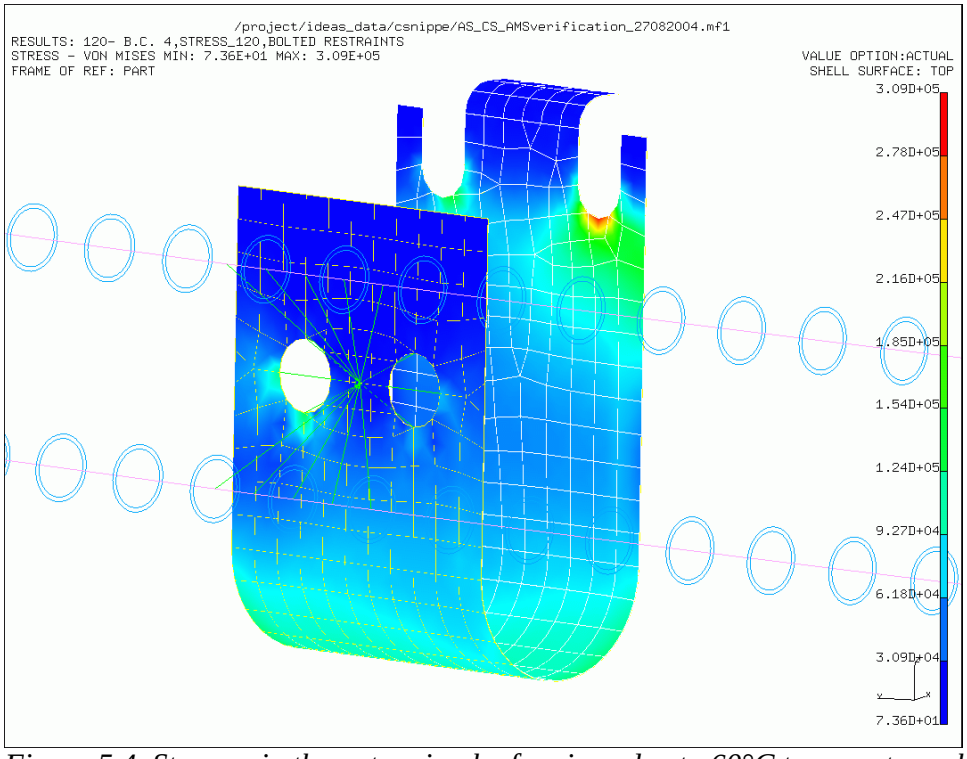

Figure 5.4. Stresses in the outer ring leaf springs due to 60°C temperature change.

6. Installation deformation

During assembly of the system, some temporary mechanical deformations will develop in the assembly. This will result in stresses, which will be released after the assembly procedure and will not add up during launching or under working conditions. These deformations, which can be put into the FE model as forced displacements, are a contraction in the cooling pipe system of 4 mm (i.e. a half loop of the cooling pipe will deform 2 mm inwards at a position halfway between the two Clamp Bases).

Before launch the vacuum case will be evacuated and deformations in the magnet flange up to 10 mm will occur. This deformation will lead to a 10 mm deformation in Z for the protruding evaporator exit tubes, see figure 6.1.

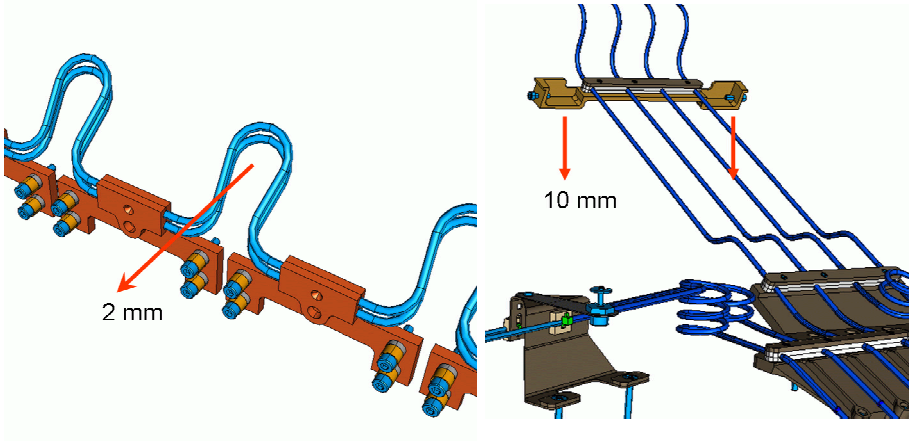

Figure 6.1. Forced, temporary, displacements during assembly.

Pushing the cooling pipes 2 mm inwards will result in a maximum stress in the cooling pipe of 36 MPa, see figure 15. As stated earlier, this stress will not add up to the stress resulting from the internal pressure of 160 bar, because this pressure will only be present after assembly of the structure.

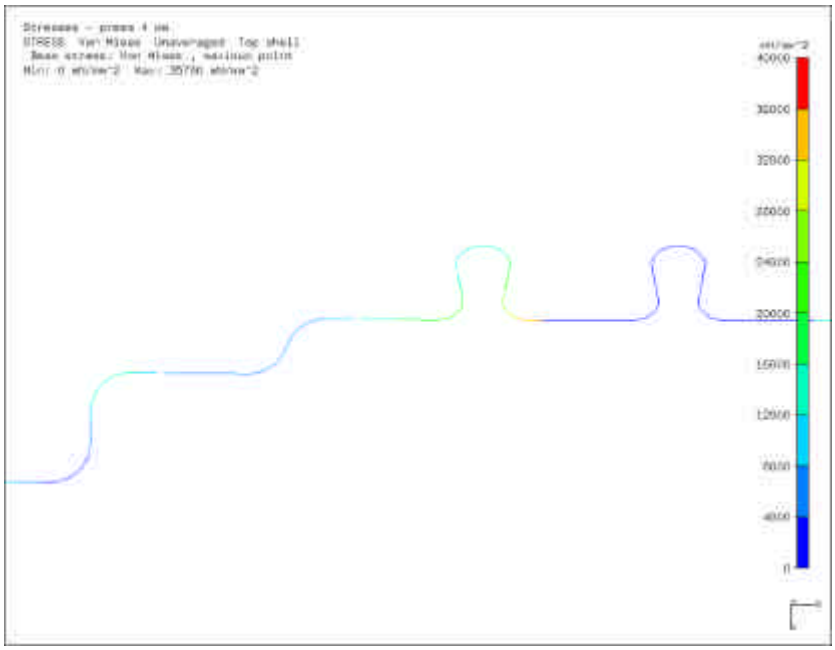

Figure 6.2. The maximum stress in the cooling pipe resulting from the 2 mm deformation is 35.8 MPa.

The displacement of the clamping block of 10 mm in a downwards direction will result in a temporary stress in the cooling pipes of 434 MPa, see figure 6.2, which might not be acceptable for this material. This deformation is present during launch, and need to be added to the acceleration stresses. The conclusion of this analyses is that the evaporator tail needs a redesign with picktails or so. (To be continued….)

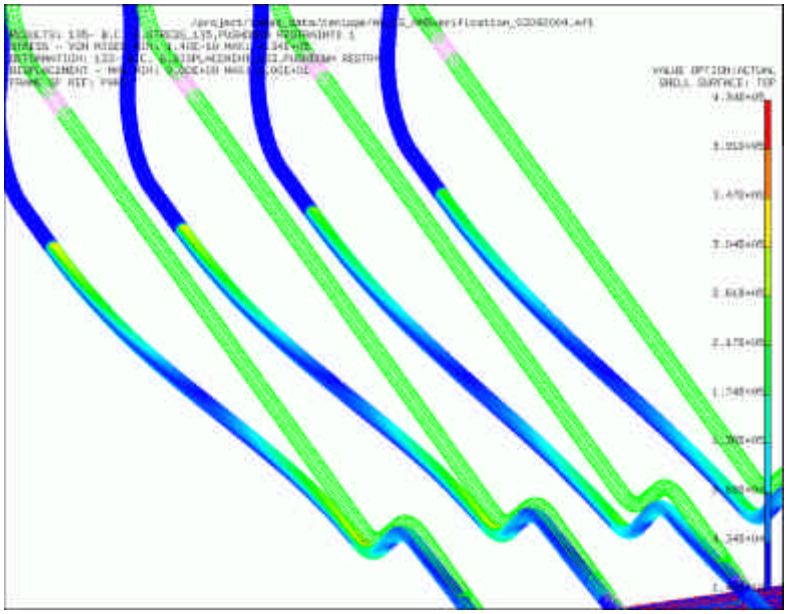

Figure 6.3. The maximum stress in the cooling pipe resulting from the 10 mm deformation is 434 MPa.

Appendix 1, Mechanical overview

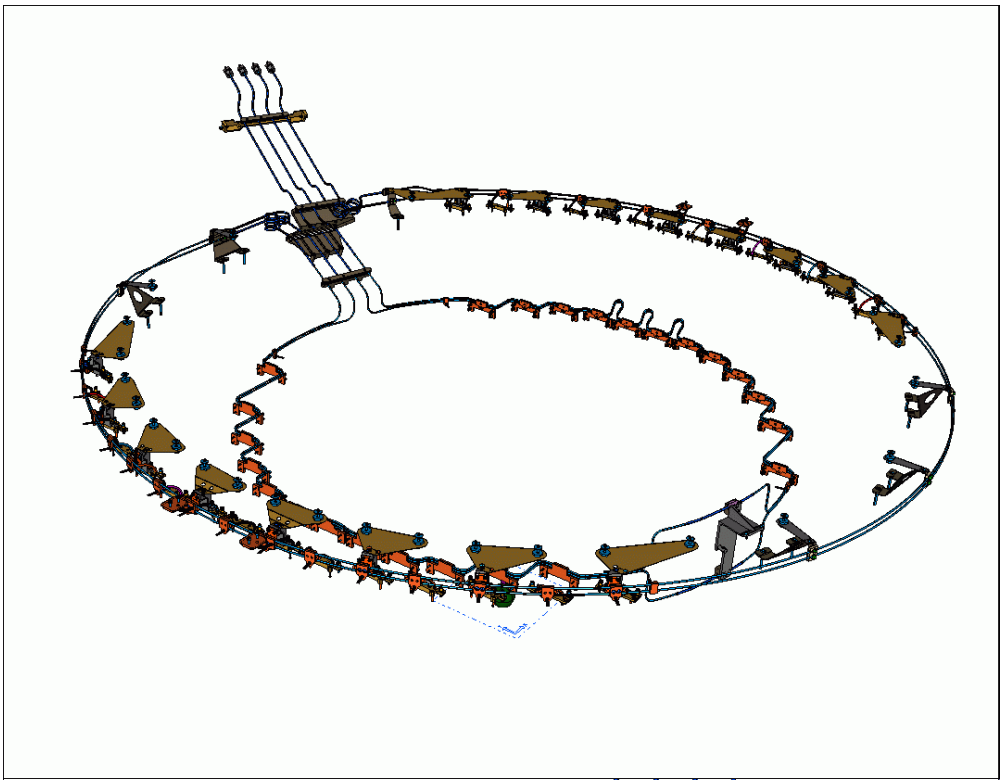

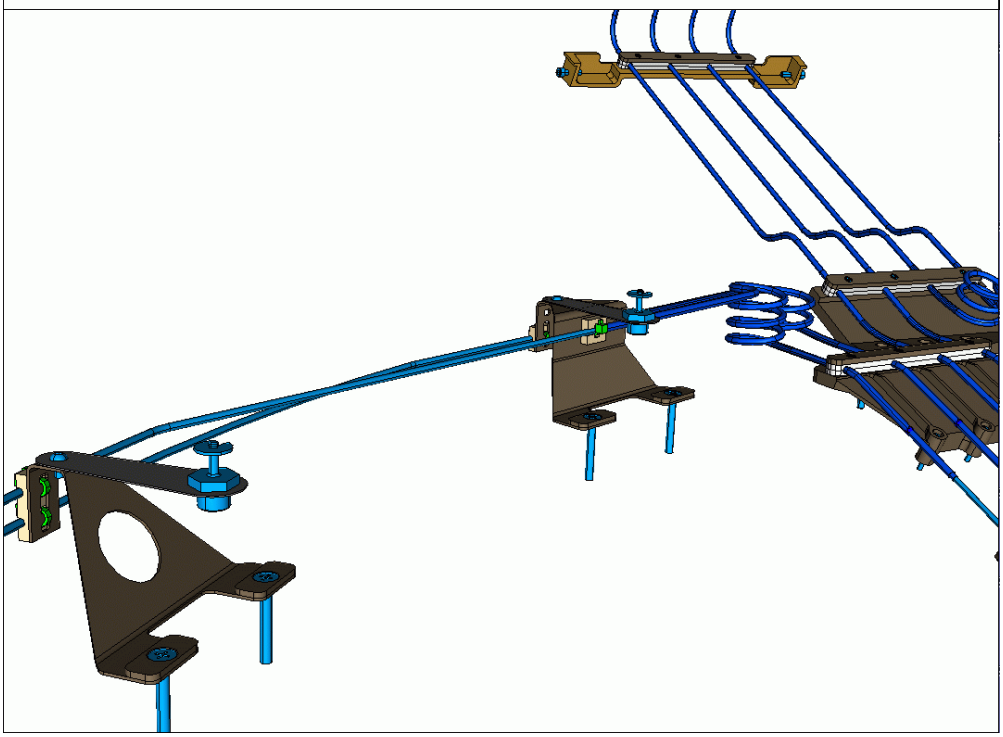

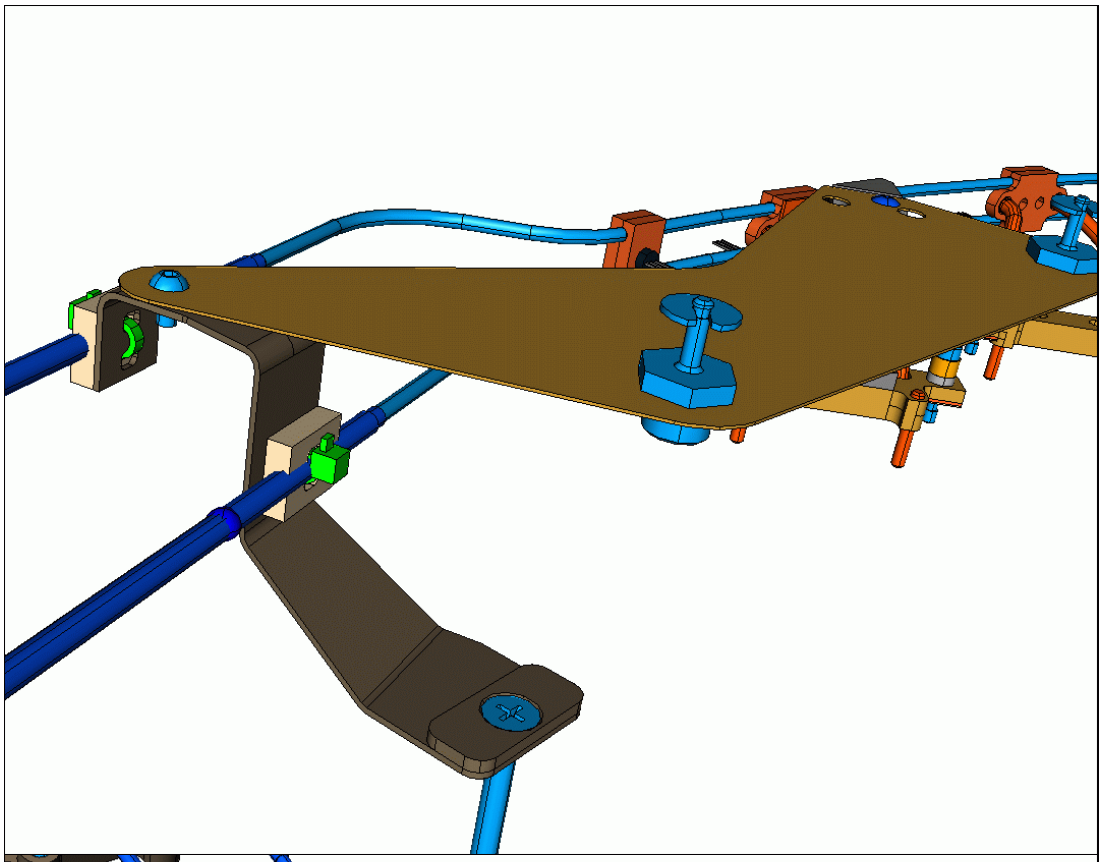

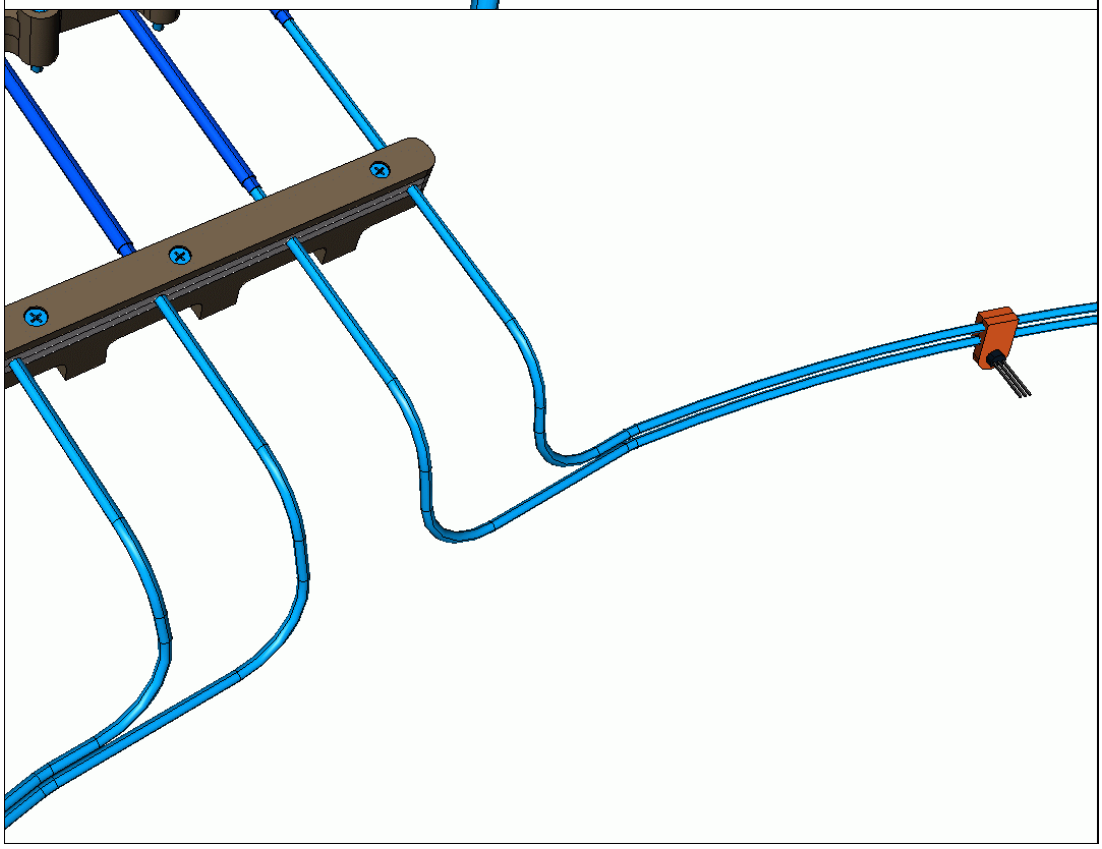

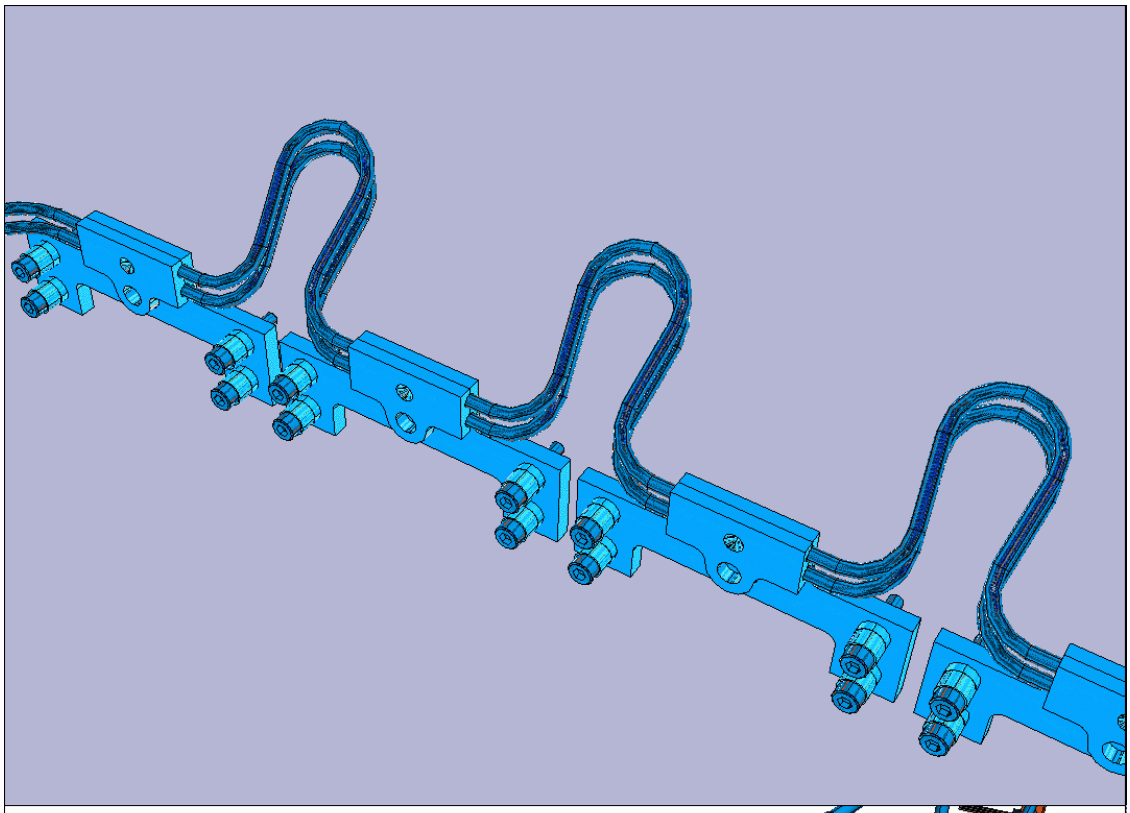

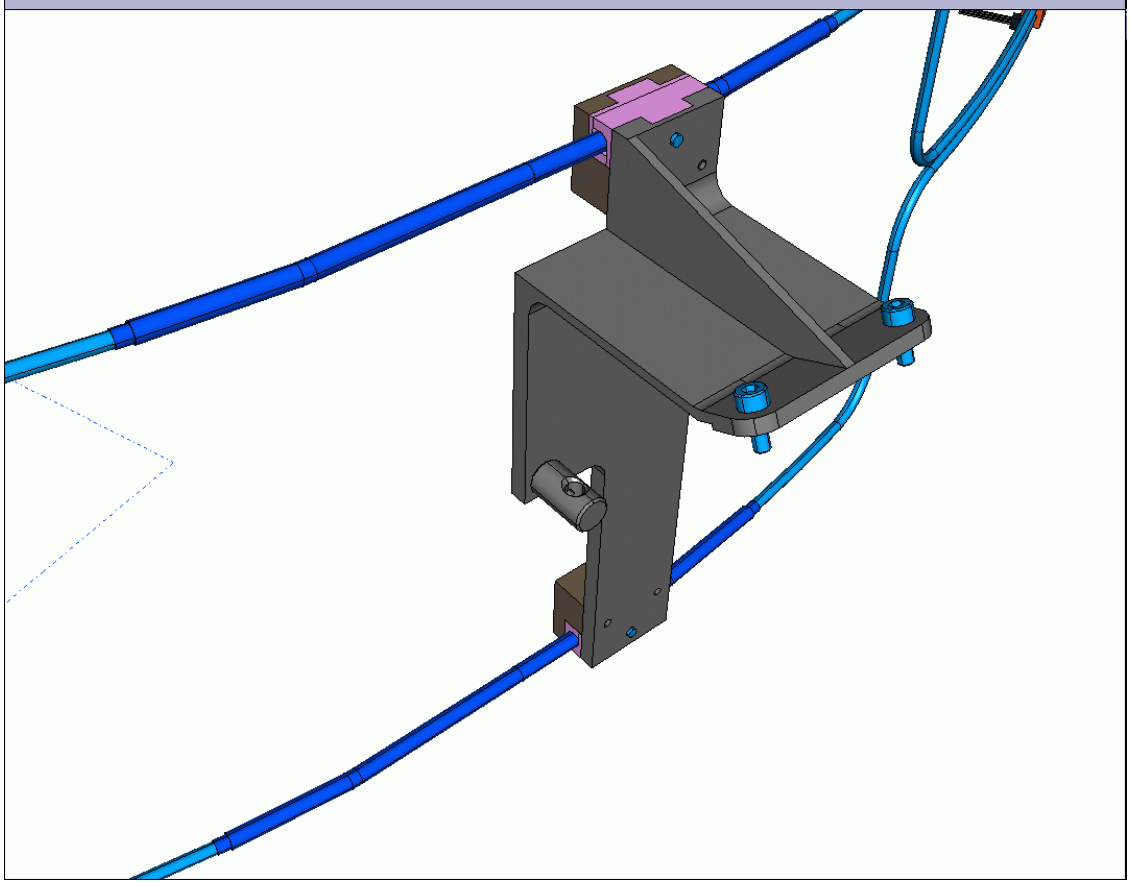

Appendix 2: Stress analyses overview

Central Evaporator clamp ASM25 Flange exit clamp ASM06

40g in x-axis

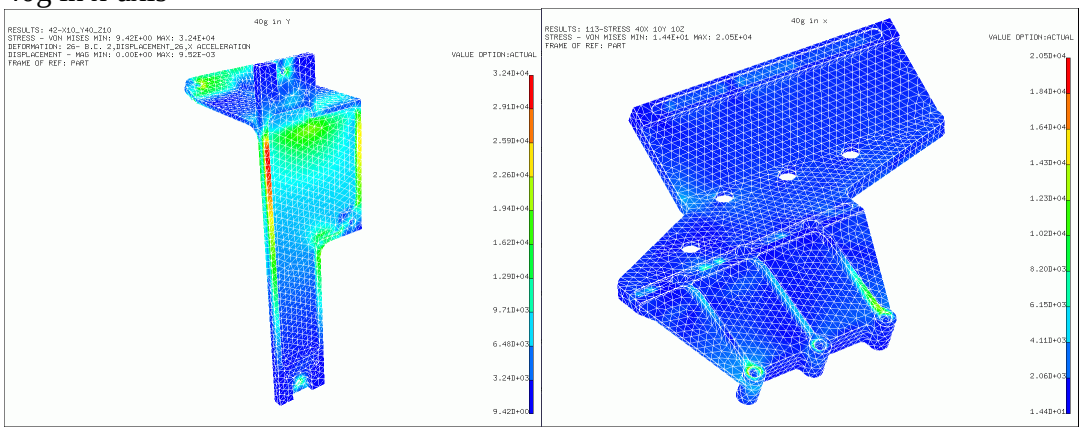

40g in Y-axis

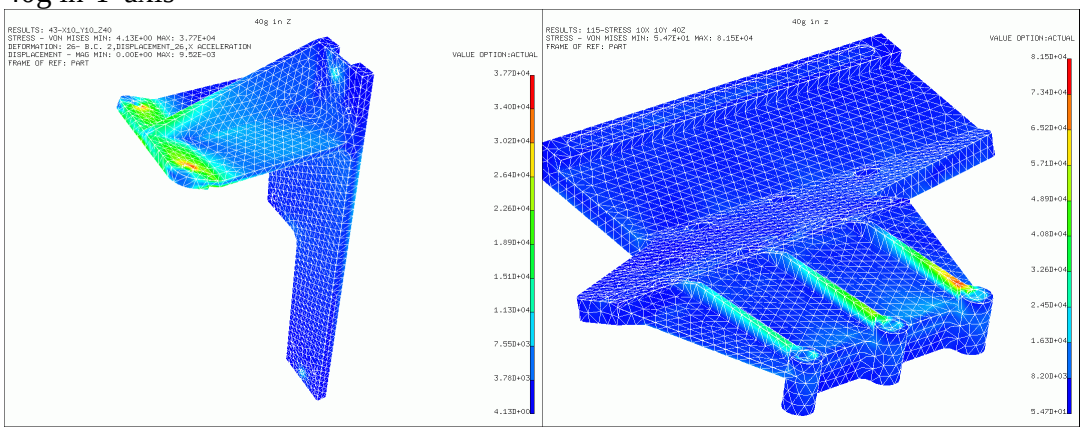

40g in Z-axis

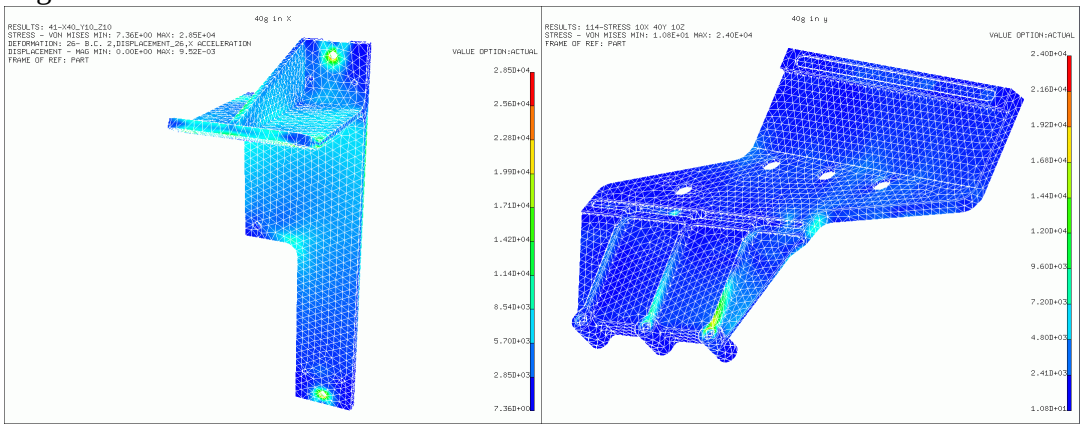

Outer ring support ASM39,ASM57

Outer ring support ASM62

40g in X-axis

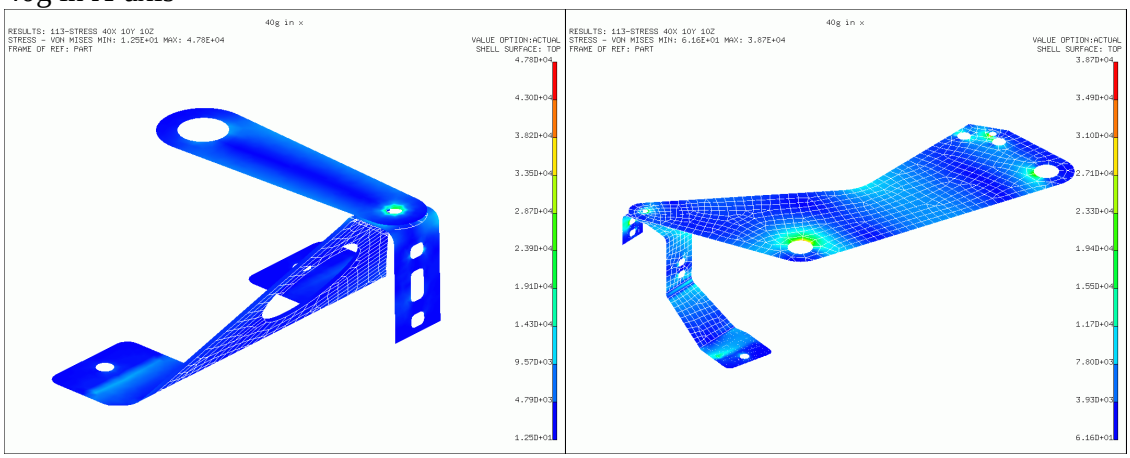

40g in Y-axis

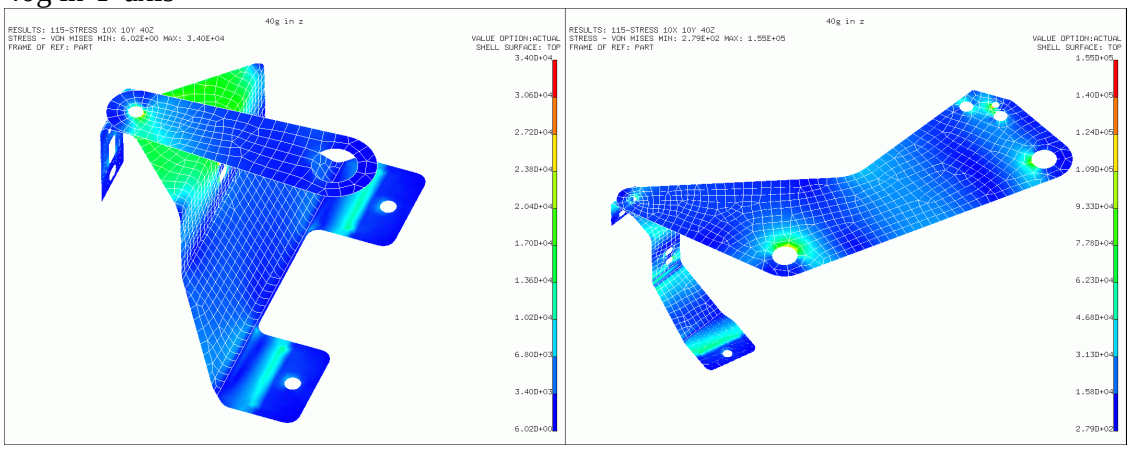

40g in Z-axis

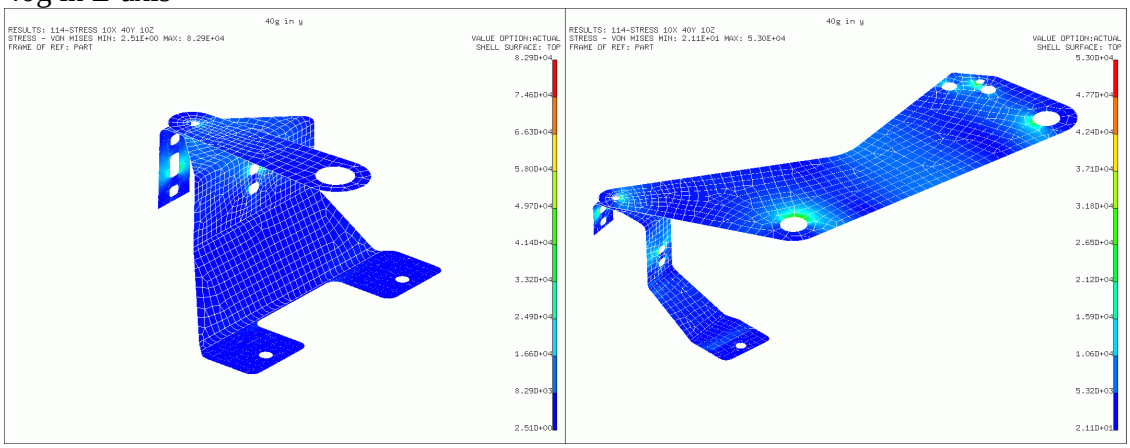

Outer ring spring support ASM1901

40g in X-axis

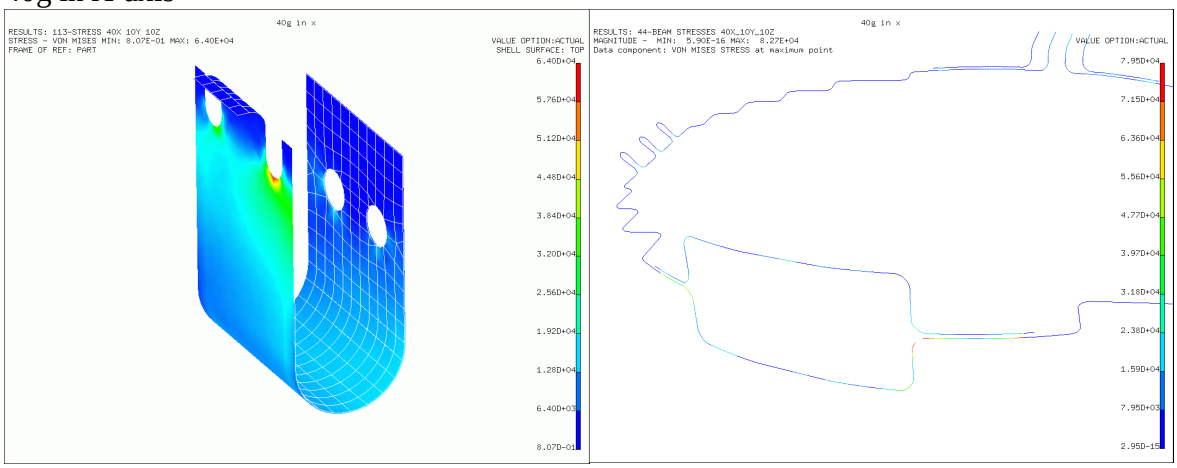

40g in Y-axis

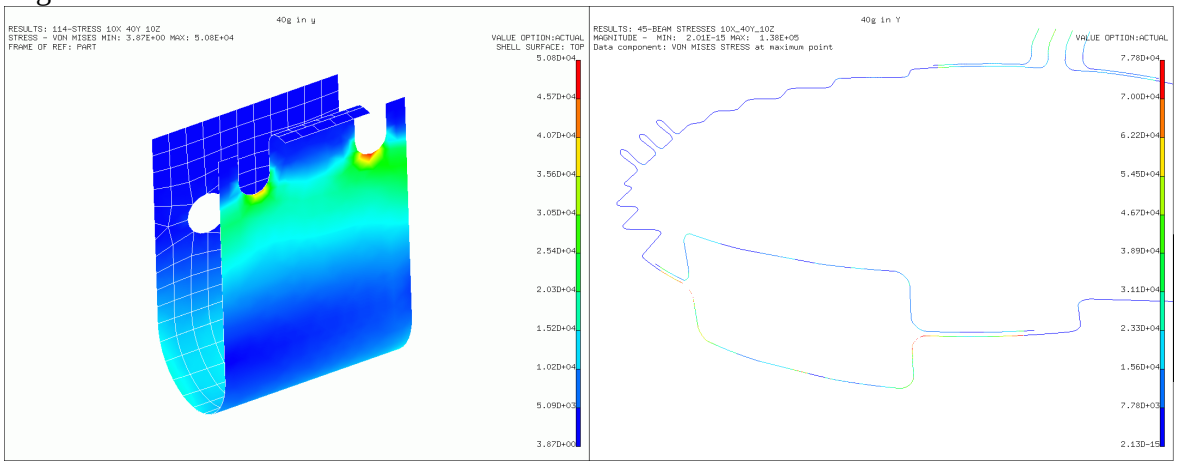

40g in Z-axis

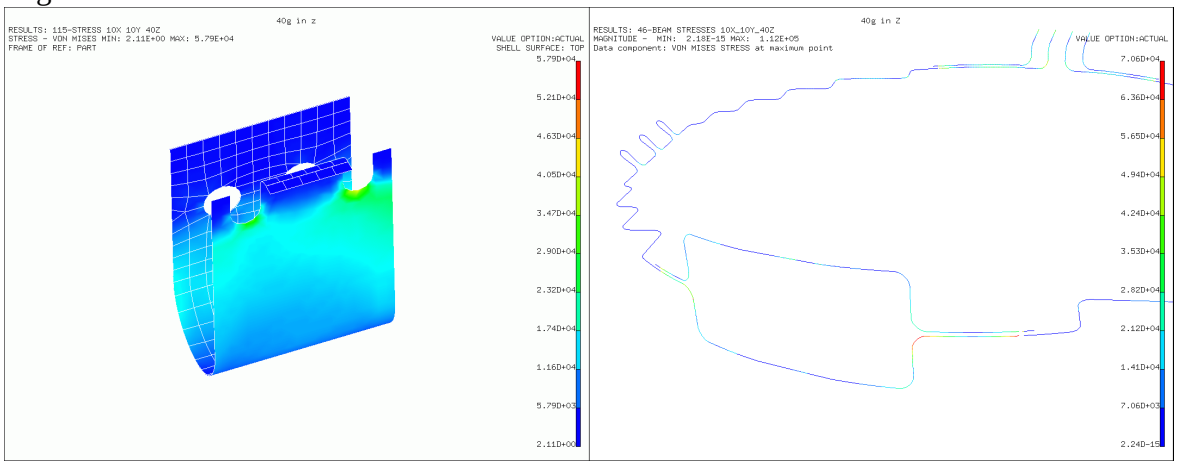

Evaporator tube (ASM28, ASM29)

40g in X-axis

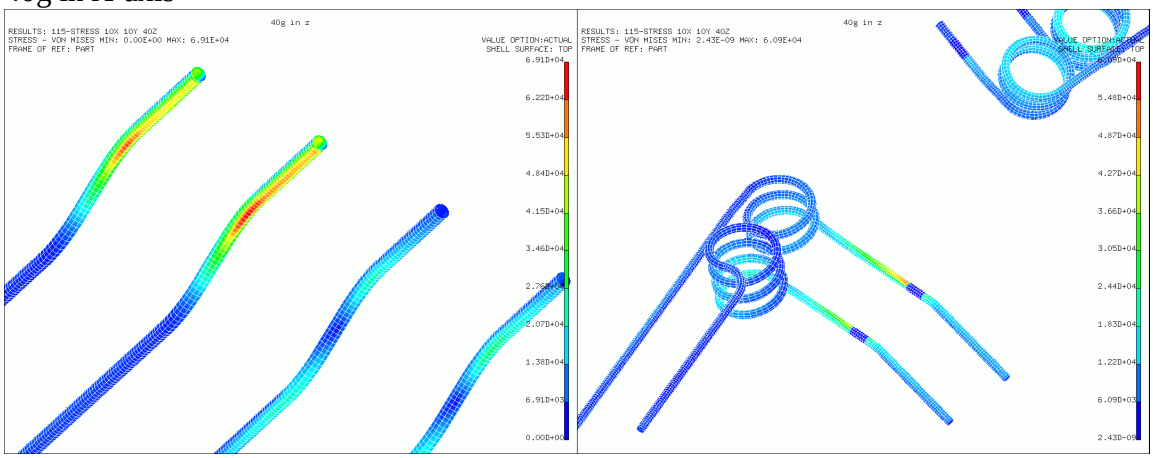

40g in Y-axis

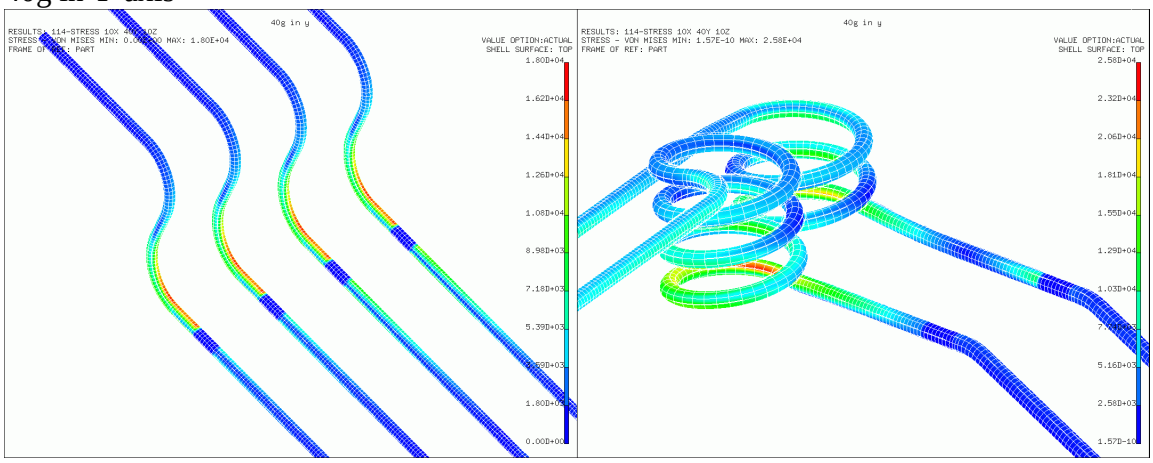

40g in Z-axis